Importance of quark interchange in pion production via nucleon-nucleon scattering

Zong-Jian Cao and W-Y. P. Hwang
Indiana University Cyclotron Facility and Nuclear Theory Center, Department of Physics, Indiana University, Bloomington, Indiana 47405
(Received 2 June 1986)

We investigate pion production via nucleon-nucleon scattering, i.e., $N+N\rightarrow N+N+\pi$, assuming that pion emission takes place *effectively* at the quark level and that quark-quark interactions are described to a reasonable approximation by one-gluon exchange plus *effective* one-pion exchange. The six-quark wave function is totally antisymmetrized. Consequently, reaction mechanisms may be grouped into several categories: (1) one-nucleon mechanism or the nucleon-only impulse approximation, (2) two-nucleon mechanisms or meson-exchange currents, and (3) reaction mechanisms involving quark interchange. Applying the formalism to the reactions $p+p\rightarrow d+\pi^+$ and $n+p\rightarrow p+p+\pi^-$, we find that, for a nucleon radius of greater than 0.8 fm (as measured in the MIT bag model), reaction mechanisms involving quark interchange may be as important as the conventional one-nucleon or two-nucleon reaction mechanisms even near the pion production threshold. This specific result provides a quantitative support of the conclusion reached by Miller and Kisslinger in the hybrid quark-baryon model concerning the necessity of incorporating quark effects in describing pion production or absorption reactions.

I. INTRODUCTION

In recent years, significant progress has been made in the quality of experimental data associated with single pion production on complex nuclei as well as via nucleon-nucleon scattering.[1] In particular, observation of high spin excited states of final nuclei in (p,π^-) reactions[2] suggests the importance of two-nucleon reaction mechanisms.

It it clear that pion production via nucleon-nucleon (NN) scattering is of special importance for unraveling the importance of the various underlying reaction mechanisms, both experimentally and theoretically. Recent experimental measurements include the data on some spin observables[3] for the $pp\rightarrow d\pi^+$ reaction and on spin-dependent cross sections[4] for the reaction $N+N\rightarrow N+N+\pi$. Meanwhile, progress in theoretical investigations of (p,π) reactions has also been made. For studying pion production on complex nuclei, several models[5] have been introduced by Keister and Kisslinger, Dillig and Conte, and Iqbal and Walker; but detailed comparison between theory and experiment remains to be carried out in such theoretical models. For studying pion production via nucleon-nucleon scattering in the intermediate-energy region near the (3,3) resonance [$\Delta(1232)$], there exist primarily two different approaches: In the first approach, which is pursued mainly by Niskanen,[6] one attempts to solve the NN-NΔ coupled equations with some assumed $NN\rightarrow N\Delta$ transition potential. This formalism has been applied to calculate spin observables for the $pp\rightarrow d\pi^+$ reaction.[6] In the second approach, which has been widely used in the literature,[7,8] one attempts to solve the Faddeev-like three-body equations, which treat the NN and NNπ systems as coupled channels. The formalism has so far been used mainly for the $pp\rightarrow d\pi^+$ reaction,[7] although there have been some recent efforts in applying this method to describing the $NN\rightarrow NN\pi$ reaction.[8] It can also be supplemented by contributions from possible dibaryon resonances without violation of the unitarity constraints.[9] All of these models[6-8] have been able to explain the gross features of the existing data reasonably well. As pointed out by Silbar,[10] however, they fail to reproduce some detailed structure of the observed data and occasionally yield even incorrect energy or angular dependences.

Recently, it has been pointed out by Miller and Kisslinger[11] that quarks may play an important role in view of the high momentum transfer involved. In particular, the typical magnitude of momentum transfer between the two nucleons in the reaction $p+p\rightarrow d+\pi^+$ is about 550 MeV/c so that the relevant distance scale is approximately 0.4 fm. This distance is much smaller than the radius of the MIT bag (~ 1.0 fm). Thus, the reaction takes place when two nucleons overlap substantially. Employing a spherical six-quark bag to approximate the NN wave functions at short distances [$r \leq r_0$ with $r_0 \sim 0.9$ fm], Miller and Kisslinger[11] investigated the reaction $p+p\rightarrow d+\pi^+$ and confirmed the important role played by quarks.

In this paper we wish to report the major results of an extensive investigation by assuming that pion emission takes place *effectively* at the quark level and that quark-quark interactions are described to a sufficiently good approximation by one-gluon exchange plus *effective* one-pion exchange. Accordingly, reaction mechanisms can be grouped into several distinct categories,[12] viz., (i) one-nucleon-mechanism (ONM) or the nucleon-only impulse approximation (NOIA), where a pion is emitted from one of the two nucleons; (ii) two-nucleon mechanisms (TNM) or meson-exchange currents (MEC), where pion emission takes place while the two nucleons exchange a pion, and here we include isobar (Δ) currents, ρ-π currents, and pair currents; (iii) reaction mechanisms involving quark inter-

change (QI) with or without one-boson exchange between the two nucleons. Such classification becomes only a phenomenological one since it is known that inclusion of pion distortions is of numerical importance and the pion-deuteron optical potential, as chosen by us to describe pion distortions, already contains the resonance behavior due to isobars [$\Delta(1232)$] and others. In practice, we choose the pion-deuteron optical potential which provides the best fit (in terms of χ^2) to the data at several incident pion energies. Thus, to avoid double counting with contributions from isobar currents, we do not include pion distortions in the ONM or NOIA contribution. In this way, we are able to carry out a parameter-free calculation for $p+p\rightarrow d+\pi^+$. Our results, as will be explained in Sec. III, support the major conclusion reached by Miller and Kisslinger[11] that, for a nucleon radius of greater than 0.8 fm, quark effects, which are identified in our formalism as contributions arising from reaction mechanisms involving quark interchange, play an important role even near threshold (where the argument regarding the large momentum transfer remains valid). Nevertheless, the optical potential for the π^-(pp) system is poorly known and this aspect presents a major uncertainty in making predictions for the $n+p\rightarrow p+p+\pi^-$ reaction.

There are also other justifiable objections to the level of the approximation which we have invoked; for instance, exchanges of more than one boson as well as couplings to other related channels have not yet been properly incorporated. However, we believe that the formalism adopted in the present work does not preclude further improvements of such kinds and may in fact serve as a reasonable starting point.

The outline of this paper is as follows. In Sec. II we describe the key ingredients of this calculation. We wish to refer interested readers to Ref. 12 for a detailed list of important formulas obtained via the present formalism. These formulas have been suitably programmed to yield sample results reported in this paper. In Sec. III we describe and discuss our major numerical results. Section IV contains a brief summary of this paper.

II. THEORY

To describe the basic ingredients of the formalism, we consider the $pp\rightarrow d\pi^+$ reaction as specified by

$$(\mathrm{pp})(p^{(i)},\zeta)\rightarrow{}^2\mathrm{H}(p^{(f)},\xi)+\phi^{\pi}(q)\ , \tag{1}$$

where $p^{(i)}$, $p^{(f)}$, and q are, respectively, the four-momenta of the initial p-p system, the deuteron, and the emitted pion in the c.m. system of the two initial protons. Further, ζ and ξ are used to characterize the intrinsic discrete degrees of freedom such as spin. For instance, ξ is the polarization four vector of the deuteron such that $\xi\cdot p^{(i)}=0$ and $\xi^*\cdot\xi=1$. Thus, the transition amplitude T_{fi} for the reaction (1) is given by

$$(2\pi)^3\delta^3(\mathbf{q}-\mathbf{p}^{(i)}+\mathbf{p}^{(f)})T_{fi}=\left\langle{}^2\mathrm{H}(\mathbf{p}^{(f)},\xi)\left|\int d^3x\,\phi^{\pi}(\mathbf{q},\mathbf{x})P_{\pi}(\mathbf{x})\right|(\mathrm{pp})(\mathbf{p}^{(i)},\zeta)\right\rangle\ . \tag{2}$$

To evaluate the matrix element appearing in Eq. (2), we may write[12]

$$P_{\pi}(\mathbf{x})=P_{\pi}^{(1)}(\mathbf{x})+P_{\pi}^{(2)}(\mathbf{x})+\cdots+P_{\pi}^{Q}(\mathbf{x})\ , \tag{3}$$

where $P_{\pi}^{Q}(\mathbf{x})$ denotes the pion source current operator due to reaction mechanisms involving quark interchange, and $P_{\pi}^{(N)}(\mathbf{x})$ is the N-body pion source current operator which acts on N constituent nucleons. In the standard treatment, $P_{\pi}^{(1)}(\mathbf{x})$ is characterized by the nucleon-only impulse approximation (NOIA) and $P_{\pi}^{(2)}(\mathbf{x})$ arises from meson-exchange currents (MEC). Specifically, the NOIA one-body pion source current $P_{\pi}^{\mathrm{NOIA}}(\mathbf{x})$ is specified by

$$P_{\pi}^{\mathrm{NOIA}}(\mathbf{x})=\sum_a\sqrt{2}\frac{g_{\pi\mathrm{NN}}}{2M}\tau_{-}^{(a)}(\boldsymbol{\sigma}^{(a)}\cdot\boldsymbol{\nabla}_x)\delta^3(\mathbf{x}-\mathbf{r}^{(a)})\ . \tag{4}$$

$$\begin{aligned}P_{\pi}^{(2)}(\mathbf{x})&\equiv P_{\pi}^{(2)}(\mathbf{x},t=0;\mathbf{r}_1,\mathbf{r}_2;\mathbf{q},E_{\pi})\\&=\int\frac{d^3k_1}{(2\pi)^3}\int\frac{d^3k_2}{(2\pi)^3}\exp[i\mathbf{k}_1\cdot(\mathbf{r}_1-\mathbf{x})+i\mathbf{k}_2\cdot(\mathbf{r}_2-\mathbf{x})]\cdot P_{\pi}^{(2)}(\mathbf{k}_1,\mathbf{k}_2;k_{10},k_{20};q,E_{\pi})\ ,\end{aligned} \tag{5}$$

with $(k_i)_{\lambda}=(p_i'-p_i)_{\lambda}$ and E_{π} the total energy of the emitted pion. The momentum-space operator $P_{\pi}^{(2)}(\mathbf{k}_1,\mathbf{k}_2,k_{10},k_{20};q,E_{\pi})$ can be represented as a sum of contributions due to the various MEC diagrams. In view of the kinematic region to be investigated, we include (1) intermediate isobar propagation (or isobar currents), (2) $(\rho\pi)$ exchange currents, and (3) "pair" currents. It is known that isobar currents play an important role at low and medium energies. Following Hwang and Walker,[13] we keep terms which are generated by a nonzero energy transfer. The NOIA and MEC diagrams considered in this paper are illustrated in Fig. 1.

As a specific example, the isobar [$\Delta(1232)$] current is given by[13]

$$
\begin{aligned}
&P_\pi^{\Delta}(\mathbf{k}_1,\mathbf{k}_2,k_{10},k_{20};\mathbf{q},E_\pi) \\
&\quad = i\frac{g_\Delta^2 f}{m_\pi^3}\sqrt{2}\left[\frac{2}{3}\tau_-^2+\frac{i}{3}(\tau^1\times\tau^2)_-\right]\boldsymbol{\sigma}^2\cdot\mathbf{k}_2(m_\pi^2+k_2^2-i\epsilon)^{-1}\cdot[M^{*2}+(p_1'+q)^2-i\epsilon]^{-1} \\
&\qquad\times\left[-\frac{3}{8}q_0k_{20}(2M^*+M)\left[1-\frac{M^2}{M^{*2}}\right]+\mathbf{k}_2\cdot\mathbf{q}\left[\frac{3}{4}M^*+\frac{5}{8}M-\frac{1}{12}\frac{M^2}{M^*}+\frac{1}{24}\frac{M^3}{M^{*2}}\right]\right. \\
&\qquad\quad\left.-i\boldsymbol{\sigma}^1\times\mathbf{k}_2\cdot\mathbf{q}\left[-\frac{M^*}{4}-\frac{3}{8}M-\frac{1}{12}\frac{M^2}{M^*}+\frac{1}{24}\frac{M^3}{M^{*2}}\right]\right] \\
&\qquad +i\frac{g_\Delta^2 f}{m_\pi^3}\sqrt{2}\left[\frac{2}{3}\tau_-^2-\frac{i}{3}(\tau^1\times\tau^2)_-\right]\boldsymbol{\sigma}^2\cdot\mathbf{k}_2(m_\pi^2+k_2^2-i\epsilon)^{-1}\cdot[M^{*2}+(p_1-q)^2-i\epsilon]^{-1} \\
&\qquad\times\left[-\frac{3}{8}q_0k_{20}(2M^*+M)\left[1-\frac{M^2}{M^{*2}}\right]+\mathbf{k}_2\cdot\mathbf{q}\left[\frac{3}{4}M^*+\frac{5}{8}M-\frac{1}{12}\frac{M^2}{M^*}+\frac{1}{24}\frac{M^3}{M^{*2}}\right]\right. \\
&\qquad\quad\left.+i\boldsymbol{\sigma}^2\times\mathbf{k}_2\cdot\mathbf{q}\left[-\frac{M^*}{4}-\frac{3}{8}M-\frac{1}{12}\frac{M^2}{M^*}+\frac{1}{24}\frac{M^3}{M^{*2}}\right]\right]+(1\leftrightarrow 2)\ . \qquad (6)
\end{aligned}
$$

Here g_Δ and f are, respectively, the $\pi N\Delta$ and πNN couplings, M, M^*, and m_π are, respectively, the nucleon, delta, and pion masses, $\{\tau_1,\tau_2,\tau_3\}$ are 2×2 Pauli matrices for isospin, and $\{\sigma_1,\sigma_2,\sigma_3\}$ are Pauli matrices for spin. The explicit expression for the $(\rho\pi)$ current or the pair current can be found in Ref. 12 or 13.

Note that we may write the pion source current operator due to reaction mechanisms involving quark interchange as follows:

$$P^{\mathcal{Q}}(\mathbf{x})=P_{14}^{\mathcal{Q}}(\mathbf{x})+P_{16}^{\mathcal{Q}}(\mathbf{x})+P_{36}^{\mathcal{Q}}(\mathbf{x})\ , \qquad (7a)$$

with

$$P_{14}^{\mathcal{Q}}(\mathbf{x})=(-12\tilde{V}_{14}^{\pi}-4\tilde{V}_{14}^{G}-12\tilde{V}_{14}^{\mathrm{OB}})\hat{P}_{36}^{\tau\sigma x} \qquad (7b)$$

and analogous expressions for $P_{16}^{\mathcal{Q}}(\mathbf{x})$ and $P_{36}^{\mathcal{Q}}(\mathbf{x})$. Here, $\hat{P}_{36}^{\tau\sigma x}$ is the exchange operator between the third and sixth quarks in isospin, spin, and coordinate space while $\tilde{V}_{14}^{\pi}$, $\tilde{V}_{14}^{G}$, and $\tilde{V}_{14}^{\mathrm{OB}}$ are, respectively, the one-pion exchange, one-gluon exchange, and one-body potentials between the first and fourth quarks.

In the present work, only S-wave and P-wave pions are considered. Thus, the initial p-p must be in the $^3P_1$ state (for S-wave pion emission), and the $^1S_0$ or $^1D_2$ state (for P-wave pion emission) because of the known $^3S_1$-$^3D_1$ wave function for the deuteron. Considering the transition from the $^3P_1$ state into the $^3S_1$-$^3D_1$ deuteron state as an illustrative example, we obtain for the NOIA amplitude,

$$T_{fi}^{\mathrm{NOIA}}(^3P_1\rightarrow{}^3S_1+{}^3D_1)=-\frac{4}{\sqrt{6}}\frac{g_{\pi NN}}{(2E_\pi)^{1/2}}\int r^2dr\frac{d\phi_s^\pi(r)}{dr}\left[v_{101}^*(r)+\frac{1}{\sqrt{2}}v_{121}^*(r)\right]v_{111}(r)\ . \qquad (8)$$

For the contribution due to isobar currents, we obtain[12,13]

$$T_{fi}^{\Delta}(^3P_1\rightarrow{}^3S_1+{}^3D_1)=-iL_1\frac{\tilde{m}_\pi^2}{4\pi}\frac{E_\pi}{(2E_\pi)^{1/2}}\int r^2dr\tilde{Y}_1(\tilde{m}_\pi r)\phi_s^\pi(r)[(\tfrac{2}{3})^{1/2}v_{101}^*(r)+(\tfrac{1}{3})^{1/2}v_{121}^*(r)]v_{111}(r)\ , \qquad (9a)$$

where L_1 and $\tilde{m}_\pi$ are specified by

$$\tilde{m}_\pi^2\equiv m_\pi^2-E_\pi^2/4 \qquad (9b)$$

and

$$L_1\equiv\frac{4}{3}i\frac{g_\Delta^2 f}{m_\pi^3}(M^{*2}-M^2-2ME_\pi-iM^*\Gamma_\Delta)^{-1}\times\left[-\frac{3}{8}\right]E_\pi(2M^*+M)\left[1-\frac{M^2}{M^{*2}}\right]\ , \qquad (9c)$$

with the energy-dependent isobar width Γ_Δ given by[14]

$$\Gamma_\Delta=\frac{0.35}{6}\frac{q^3}{m_\pi^2}\frac{(M^*+M)^2-m_\pi^2}{M^{*2}}\left[1-\frac{E_\pi}{2(M+E_\pi)}\right]^3\ . \qquad (9d)$$

Further, $\tilde{Y}_1(mr)$ is an "extended" Yukawa function as defined by

$$\frac{m}{4\pi}\tilde{Y}_0(mr)\equiv\int\frac{d^3k}{(2\pi)^3}\frac{\exp(i\mathbf{k}\cdot\mathbf{r})}{\mathbf{k}^2+m^2-i\epsilon}\ , \tag{9e}$$

and

$$\tilde{Y}_1(mr)=-\frac{1}{m}\frac{d\tilde{Y}_0(mr)}{dr}\ . \tag{9f}$$

In Eqs. (9e) and (9f), $m^2\leq 0$ is allowed. The two-nucleon radial wave functions, $v_{101}(r)$, $v_{111}(r)$, and $v_{121}(r)$, are generated using the Reid soft-core potential.

The partial-wave amplitude from initial $^3P_1$ ($M=0$) to final $^3S_1$ ($M'=0$) due to the $V^{\pi}_{14}\hat{P}_{36}$ interaction may be obtained as follows:

$$T^{\pi}_{14}(^3P_1\rightarrow{}^3S_1)=\int d^3r v^{*}_{101}(r)\chi^{\dagger}_{10}(4\pi)^{-1/2}\eta^{\dagger}_{10}\left[\int d^3x\,\phi^{\pi}(\mathbf{q},\mathbf{x})\tilde{V}^{\pi}_{14}\hat{P}^{\tau\sigma x}_{36}\right](\tfrac{1}{2})^{1/2}$$
$$\times[Y_{11}(\hat{\mathbf{r}})\chi_{1-1}-Y_{1-1}(\hat{\mathbf{r}})\chi_{11}]v_{111}(r)\eta_{11}\ , \tag{10}$$

with χ_{10}, $\chi_{1,\pm1}$ the $S=1$ spin wave functions and η_{10},η_{11} the $I=1$ isospin wave functions of the two nucleons. Simplifying the algebra related to spin and isospin, we obtain

$$T^{\pi}_{14}(^3P_1\rightarrow{}^3S_1)=\int d^3r v^{*}_{101}(r)v_{111}(r)\frac{1}{4\sqrt{2\pi}}[Y_{11}(\hat{r})-Y_{1-1}(\hat{r})]$$
$$\times\left[\left\langle \mathrm{p}(\uparrow)\mathrm{n}(\downarrow)-\mathrm{n}(\uparrow)\mathrm{p}(\downarrow)\right|\int d^3x\,\phi^{\pi}(\mathbf{q},\mathbf{x})\tilde{V}^{\pi}_{14}\hat{P}^{\tau\sigma x}_{36}\left|\mathrm{p}(\uparrow)\mathrm{p}(\uparrow)\right\rangle\right.$$
$$\left.+\left\langle \mathrm{p}(\downarrow)\mathrm{n}(\uparrow)-\mathrm{n}(\downarrow)\mathrm{p}(\uparrow)\right|\int d^3x\,\phi^{\pi}(\mathbf{q},\mathbf{x})\tilde{V}^{\pi}_{14}\hat{P}^{\tau\sigma x}_{36}\left|\mathrm{p}(\uparrow)\mathrm{p}(\uparrow)\right\rangle\right]\ . \tag{11}$$

Here the quantity $\tilde{V}^{\pi}_{14}$ is to be specified explicitly by Eq. (18a) given later. We may relate the spin amplitudes at the nucleon level to those defined at the quark level.[12] For instance, we have

$$(\sqrt{6})^4\langle \mathrm{p}(\uparrow)\mathrm{n}(\downarrow)\,|\,\tilde{V}^{\pi}_{14}\hat{P}^{\tau\sigma x}_{36}\,|\,\mathrm{p}(\uparrow)\mathrm{p}(\uparrow)\rangle$$
$$=\tfrac{1}{9}\eta^2(\,13f^{\pi}_4+23f^{\pi^*}_4+20f^{\pi}_5$$
$$-38f^{\pi}_6+15f^{\pi^*}_6-16f^{\pi}_7+39f^{\pi^*}_7)\ , \tag{12a}$$

$$(\sqrt{6})^4\langle \mathrm{n}(\uparrow)\mathrm{p}(\downarrow)\,|\,\tilde{V}^{\pi}_{14}\hat{P}^{\tau\sigma x}_{36}\,|\,\mathrm{p}(\uparrow)\mathrm{p}(\uparrow)\rangle$$
$$=\tfrac{1}{9}\eta^2(12f^{\pi}_4-8f^{\pi^*}_4-6f^{\pi}_5+2f^{\pi^*}_5$$
$$+9f^{\pi}_6-2f^{\pi^*}_6-7f^{\pi^*}_7)\ , \tag{12b}$$

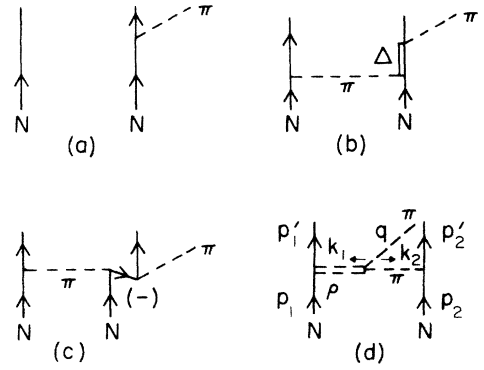

FIG. 1. Intercluster reaction mechanisms, including pion production arising from (a) nucleon only impulse approximation (NOIA), (b) isobar currents, (c) pair current, and (d) $(\rho\pi)$-exchange current.

$$(\sqrt{6})^4\langle \mathrm{p}(\downarrow)\mathrm{n}(\uparrow)\,|\,\tilde{V}^{\pi}_{14}\hat{P}^{\tau\sigma x}_{36}\,|\,\mathrm{p}(\uparrow)\mathrm{p}(\uparrow)\rangle$$
$$=\tfrac{1}{9}\eta^2(2f^{\pi}_4-6f^{\pi^*}_4-8f^{\pi}_5+12f^{\pi^*}_5$$
$$+7f^{\pi}_6+2f^{\pi}_7-9f^{\pi^*}_7)\ , \tag{12c}$$

$$(\sqrt{6})^4\langle \mathrm{n}(\downarrow)\mathrm{p}(\uparrow)\,|\,\tilde{V}^{\pi}_{14}\hat{P}^{\tau\sigma x}_{36}\,|\,\mathrm{p}(\uparrow)\mathrm{p}(\uparrow)\rangle$$
$$=\tfrac{1}{9}\eta^2(20f^{\pi^*}_4+39f^{\pi}_5+f^{\pi^*}_5-39f^{\pi}_6$$
$$+16f^{\pi^*}_6-15f^{\pi}_7+38f^{\pi^*}_7)\ . \tag{12d}$$

Here η stands for the overlap integral defined by

$$\eta\equiv\langle u_B(\downarrow)\,|\,u_A(\downarrow)\rangle\ . \tag{13}$$

To obtain Eqs. (12a)–(12d), we have introduced the various QQ amplitudes listed below:

$$f^{\pi}_1=\langle u(\uparrow)u(\uparrow)\,|\,\hat{V}^{\pi}_{14}\,|\,u(\uparrow)u(\uparrow)\rangle\ , \tag{14a}$$

$$f^{\pi}_2=\langle u(\uparrow)u(\downarrow)\,|\,\hat{V}^{\pi}_{14}\,|\,u(\uparrow)u(\downarrow)\rangle\ , \tag{14b}$$

$$f^{\pi}_3=\langle u(\downarrow)u(\uparrow)\,|\,\hat{V}^{\pi}_{14}\,|\,u(\uparrow)u(\downarrow)\rangle\ , \tag{14c}$$

$$f^{\pi}_4=\langle u(\uparrow)u(\downarrow)\,|\,\hat{V}^{\pi}_{14}\,|\,u(\uparrow)u(\uparrow)\rangle\ , \tag{14d}$$

$$f^{\pi}_5=\langle u(\downarrow)u(\uparrow)\,|\,\hat{V}^{\pi}_{14}\,|\,u(\uparrow)u(\uparrow)\rangle\ , \tag{14e}$$

$$f^{\pi}_6=\langle u(\uparrow)u(\uparrow)\,|\,\hat{V}^{\pi}_{14}\,|\,u(\uparrow)u(\downarrow)\rangle\ , \tag{14f}$$

$$f^{\pi}_7=\langle u(\downarrow)u(\downarrow)\,|\,\hat{V}^{\pi}_{14}\,|\,u(\uparrow)u(\downarrow)\rangle\ , \tag{14g}$$

$$f^{\pi}_8=\langle u(\downarrow)u(\downarrow)\,|\,\hat{V}^{\pi}_{14}\,|\,u(\uparrow)u(\uparrow)\rangle\ . \tag{14h}$$

All f's with a star are defined by replacing $\hat{V}_{ij}$ with $\hat{V}_{ji}$ in the f's; for example,

$$f_2^{\pi^*} = \langle u(\uparrow)u(\downarrow) \mid \hat{V}_{41}^{\pi} \mid u(\uparrow)u(\downarrow) \rangle \ . \tag{15}$$

The operator $\hat{V}_{14}^{\pi}$ is related to $\tilde{V}_{14}^{\pi}$ via Eq. (18b) to be given later. We may substitute any of the u quarks by a d quark in Eqs. (13) and (14a)–(14h) because of the assumption of the equality of the mass of the up and down quarks. Using Eqs. (12a)–(12d), we obtain from Eq. (11)

$$T_{14}^{\pi}({}^3P_1 \to {}^3S_1) = -\frac{\sqrt{3}}{288\pi}\frac{1}{9}\int r^2 dr\, \eta^2 v_{101}^*(r) v_{111}(r) \int d\Omega \sin\theta \cos\phi (\, 3f_4^{\pi} + 5f_4^{\pi^*} - 21f_5^{\pi} + 13f_5^{\pi^*} - f_6^{\pi} + f_6^{\pi^*} + f_7^{\pi} - f_7^{\pi^*}) \ . \tag{16}$$

This procedure may be applied to the other transition channels as well as to the quark amplitudes due to $\tilde{V}_{16}^{\pi}\hat{P}_{36}$ and $\tilde{V}_{36}^{\pi}\hat{P}_{36}$ for various initial and final two-nucleon states. Contributions obtained in this way should be added directly to the NOIA and MEC amplitudes, which are obtained in a way described earlier. A complete list of the formulas for the NOIA, MEC, and QI transition amplitudes [which are analogous to Eqs. (8), (9a), and (16)] suitable for both the reactions $p + p \to d + \pi^+$ and $n + p \to p + p + \pi^-$ can be found in Ref. 12.

An important task has to do with simplification of the various quark-quark (QQ) transition amplitudes, which consist of integrals of high dimension. To this end, we wish to invoke a relativistic quark model to demonstrate the feasibility of carrying out these high-dimensional integrals. As an illustrative example, we consider the quark-quark amplitude $f_j^{\pi}(\mathbf{r},s)$ due to the $\tilde{V}_{14}^{\pi}\hat{P}_{36}$ interaction which is specified (for $1 \le j \le 8$) by

$$f_j^{\pi}(\mathbf{r};s) = \int d^3r_1 d^3r_4 [\psi^{\dagger}(\mathbf{r}_1 - \mathbf{r}/2)\psi^{\dagger}(\mathbf{r}_4 + \mathbf{r}/2)] \times \int \frac{d^3k_1}{(2\pi)^3} \int \frac{d^3k_4}{(2\pi)^3} \exp(i\mathbf{k}_1\cdot\mathbf{r}_1 + i\mathbf{k}_4\cdot\mathbf{r}_4) \times \int d^3x \phi^{\pi}(\mathbf{x}) \exp[-i\mathbf{x}\cdot(\mathbf{k}_1 + \mathbf{k}_4)] \cdot \hat{V}_{14}^{\pi}[\psi(\mathbf{r}_4 + \mathbf{r}/2)\psi(\mathbf{r}_1 - \mathbf{r}/2)] \ . \tag{17}$$

Here $\mathbf{r}_1$ and $\mathbf{r}_4$ are, respectively, the coordinates of the first and fourth quarks with respect to the common origin O as depicted in Fig. 2. We note that the center-to-center $\mathbf{r}$ and the relative instantaneous cluster velocity $\mathbf{v}$ are also indicated in this figure. We also note that the quarks 1, 2, and 3 are assumed in cluster B and the quarks 4, 5, and 6 in cluster A initially. To specify the interaction $\hat{V}_{14}^{\pi}$ appearing in Eq. (17), we apply Feynman's rules to the diagrams illustrated by Fig. 3 and obtain

$$\tilde{V}_{ij}^{(\pi)} = (-i)\left[-g_{Q\pi}\gamma_4\gamma_5\tau^k \frac{\phi^k}{\sqrt{2E_{\pi}}}\frac{1}{i}\frac{m + i\gamma(p'+q)}{m^2 + (p'+q)^2 - i\epsilon}(-g_{Q\pi}\gamma_5\tau^J)\right]^{(i)} \frac{1}{i}\frac{1}{k_j^2 + m_{\pi}^2 - i\epsilon}(-g_{Q\pi}\gamma_4\gamma_5\tau^J)^{(j)} + (-i)\left[-g_{Q\pi}\gamma_4\gamma_5\tau^k \frac{\phi^k}{\sqrt{2E_{\pi}}}\frac{1}{i}\frac{m + i\gamma(p-q)}{m^2 + (p-q)^2 - i\epsilon}(-g_{Q\pi}\gamma_5\tau^J)\right]^{(i)} \frac{1}{i}\frac{1}{k_j^2 + m_{\pi}^2 - i\epsilon}(-g_{Q\pi}\gamma_4\gamma_5\tau^J)^{(j)} + \{i \leftrightarrow j\} \ , \tag{18a}$$

which can be rewritten as follows:

$$\tilde{V}_{ij}^{\pi} = \hat{V}_{ij}^{\pi}(\tau_+^j + \tau_3^i\tau_+^j - \tau_+^i\tau_3^j) + \hat{V}_{ji}^{\pi}(\tau_+^i + \tau_3^j\tau_+^i - \tau_+^j\tau_3^i) \ , \tag{18b}$$

with

$$\tau_+ \equiv \tfrac{1}{2}(\tau_1 + i\tau_2) \ . \tag{18c}$$

After stripping off the color factor [as required from the derivation of Eq. (7b)] and the isospin factor [from Eqs. (12a)–(12d)], we obtain the one-pion exchange potential between two quarks,

$$\hat{V}_{ij}^{\pi} = (g_{Q\pi}\gamma_4\gamma_5)^{(j)} \frac{1}{k_j^2 + m_{\pi}^2 - i\epsilon} \times \left\{(-i)g_{Q\pi}^2\gamma_4\gamma_5 \frac{1}{(2E_{\pi})^{1/2}} \times \left[\frac{m + i\gamma(p'+q)}{m^2 + (p'+q)^2 - i\epsilon} + \frac{m + i\gamma(p-q)}{m^2 + (p-q)^2 - i\epsilon}\right]\gamma_5\right\}^{(i)} \ , \tag{19a}$$

and the one-gluon exchange potential between two quarks,

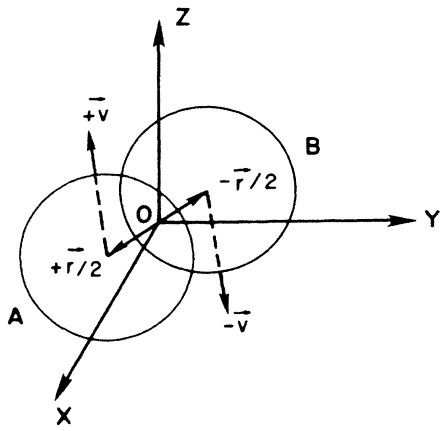

FIG. 2. Coordinate system chosen for calculating quark-quark amplitudes. The middle point of the separation between two clusters is chosen as the origin of the coordinates.

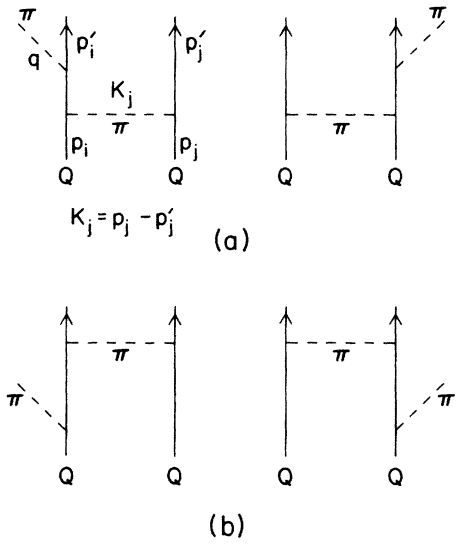

FIG. 3. Pion production mechanisms at the quark level. Here, only two-body mechanisms with one-pion exchange between quarks are shown.

$$\hat{V}_{ij}^{G}=(g_{QG}\gamma_4\gamma_\lambda)^{(j)}\frac{1}{k_j^2+m_\pi^2-i\epsilon}\times\left\{(-i)g_{QG}g_{Q\pi}\gamma_4\frac{1}{(2E_\pi)^{1/2}}\times\left[\gamma_5\frac{m+i\gamma(p'+q)}{m^2+(p'+q)^2-i\epsilon}\gamma_\lambda+\gamma_\lambda\frac{m+i\gamma(p-q)}{m^2+(p-q)^2-i\epsilon}\gamma_5\right]\right\}^{(i)}. \tag{19b}$$

The one-body potential $\hat{V}_i^{\mathrm{OB}}$ is defined by

$$\hat{V}_i^{\mathrm{OB}}=2ig_{Q\pi}(\gamma_4\gamma_5)^{(i)}\delta^3(\mathbf{x}-\mathbf{r}^{(i)}) . \tag{19c}$$

Substituting (Eq. (9a) into Eq. (17) and carrying out the integration first over d^3k_1 and then over d^3x, we find

$$f_j^\pi(\mathbf{r};s)=\int\frac{d^3k_4}{(2\pi)^3}\frac{1}{k_4^2+m_\pi^2-i\epsilon}\left[\int d^3r_4\psi^\dagger(\mathbf{r}_4+\mathbf{r}/2)(g_{Q\pi}\gamma_4\gamma_5)\psi(\mathbf{r}_4+\mathbf{r}/2)\exp(-i\mathbf{k}_4\cdot\mathbf{r}_4)\right]\times\left\{\int d^3r_1\psi^\dagger(\mathbf{r}_1-\mathbf{r}/2)(-i)g_{Q\pi}^2\gamma_4\gamma_5(2E)^{-1/2}\left[\frac{m+i\gamma(p'+q)}{m^2+(p'+q)^2-i\epsilon}+\frac{m+i\gamma(p-q)}{m^2+(p-q)^2-i\epsilon}\right]\times\gamma_5\psi(\mathbf{r}_1-\mathbf{r}/2)\phi^{(\pi)}(\mathbf{r}_1)\exp(i\mathbf{k}_4\cdot\mathbf{r}_1)\right\} . \tag{20}$$

To simplify this complicated expression, we invoke the quark wave function which is obtained from the Dirac equation with the confining potentials U and V_0, viz.,

$$[\gamma\cdot\nabla+\gamma_4(E-V_0)]\psi(\mathbf{r})+(U+m)\psi(\mathbf{r})=0 . \tag{21}$$

We may write

$$\psi(\mathbf{r})=\begin{bmatrix}g(\mathbf{r})\\h(\mathbf{r})\end{bmatrix}, \tag{22a}$$

and choose

$$V_0-U=a ,\qquad V_0=\tfrac{1}{2}kr^2 , \tag{22b}$$

with a and k constants, so that

$$\psi(\mathbf{r},s)=N\exp(-r^2/R^2)\begin{bmatrix}1\\i\zeta\sigma\cdot\mathbf{r}\end{bmatrix}\exp(-iEt)\chi_s . \tag{23}$$

TABLE I. Comparison between the radius parameter R and the MIT bag radius R_M. The calculated $\langle r^2 \rangle$ and the lowest eigenenergy are set equal to each other for our model and the MIT bag model in obtaining these numbers. In both cases, a massless quark is assumed.

R (fm)	0.286	0.357	0.429	0.500	0.572	0.643	0.714	0.786	0.857
R_M (fm)	0.4	0.5	0.6	0.7	0.8	0.9	1.0	1.1	1.2

Here ζ and N are given by

$$\zeta = \frac{2}{R^2(E+m-a)} , \tag{24a}$$

with E and m the total energy and mass of the quark, and

$$N = \left[\frac{2\sqrt{2}}{R^3 \pi \sqrt{\pi}} \left[1 + \frac{3}{R^2(E+m-a)^2} \right]^{-1} \right]^{1/2} , \tag{24b}$$

where the constant a is given by

$$a = E + (m + 6/R^2)^{1/2} . \tag{24c}$$

We use this wave function to approximate that of the MIT bag model[15] by choosing R such that the average values of r^2 and the lowest eigenenergy are the same as those given in the MIT bag model.[15] In Table I we list the corresponding values of R in the MIT bag model for different radii in the present model, assuming massless quarks. In the present model the overlap integral η as defined by Eq. (13) is given by

$$\begin{aligned} \eta &\equiv \langle u_A(\uparrow) \mid u_B(\downarrow) \rangle \\ &= \int d^3 r_3 \psi^\dagger(\mathbf{r}_3 - \mathbf{r}/2) \psi(\mathbf{r}_3 + \mathbf{r}/2) \\ &= N^2 \exp(-r^2/2R^2) R^3 (\pi/2)^{3/2} \\ &\quad \times (1 - \zeta^2 r^2/4 + 3\zeta^2 R^2/4) . \end{aligned} \tag{25}$$

To evaluate a QQ amplitude such as that specified by Eq. (20), we allow the momentum operators appearing in the quark propagators, $\mathbf{p}'$ and $\mathbf{p}$, to act on either the final or initial quark wave function. By Fourier transforming the quark wave function into momentum space, allowing the momentum operator to act on the momentum-space wave function, and then Fourier transforming the result back into configuration space, we find

$$N_1 \exp[-(\mathbf{r}_1 - \mathbf{r}/2)^2/R^2][1, -i\zeta \boldsymbol{\sigma} \cdot (\mathbf{r}_1 - \mathbf{r}/2)] \frac{1}{m^2 + (p'+q)^2 - i\epsilon} = N_1 \left[u_D^\dagger(\mathbf{r}_1 - \mathbf{r}/2), i\frac{\zeta R^2}{2} \boldsymbol{\sigma} \cdot \nabla_{r_1} u_D^\dagger(\mathbf{r}_1 - \mathbf{r}/2) \right] , \tag{26a}$$

with $u_D^\dagger(\mathbf{r}_1 - \mathbf{r}/2)$ given by

$$\begin{aligned} u_D^\dagger(\mathbf{r}_1 - \mathbf{r}/2) \equiv N_1 \int d^3 r' \exp(-i\mathbf{q} \cdot \mathbf{r}') \\ \times \exp\left[-\frac{(\mathbf{r}_1 - \mathbf{r}/2 + \mathbf{r}')^2}{R^2} \right] \\ \times \frac{m_+}{4\pi} \tilde{Y}_0(m_+ r') . \end{aligned} \tag{26b}$$

Here m_+ is given by

$$m_+^2 = m^2 - (E_f + E_\pi)^2 , \tag{27}$$

with E_f and m the final total energy and mass of the quark, and E_π and $\mathbf{q}$ the total energy and the three momentum of the emitted pion. The extended Yukawa function, $\tilde{Y}_0(m_+ r')$, is defined by Eq. (9e) given earlier. Exactly the same procedure can be performed with the initial quark wave function. We obtain the same result as in Eqs. (26) except that m_+ is replaced by m_- as defined by

$$m_-^2 = m^2 - (E_i - E_\pi)^2 , \tag{28}$$

with E_i the initial total energy of the quark. Note that the integrals appearing in Eq. (26b) can easily be carried out numerically. Typical numerical results are illustrated in Figs. (4a)—(4b), where $u_D^\dagger(\mathbf{r}_1 - \mathbf{r}/2)$ is shown as a function of the absolute value, $|\mathbf{r}_1 - \mathbf{r}/2|$, or of the angle θ between $\mathbf{r}_1 - \mathbf{r}/2$ and $\mathbf{q}$. This function vanishes almost completely for both real and imaginary parts as $|\mathbf{r}_1 - \mathbf{r}/2|$ is close to $2R$. We also note that derivatives of $u_D^\dagger(\mathbf{r}_1 - \mathbf{r}/2)$ can also be evaluated numerically in an analogous fashion. For instance, we have

$$\begin{aligned} \nabla_{r_1} u_D^\dagger(\mathbf{r}_1 - \mathbf{r}/2) = -2/R^2 [(\mathbf{r}_1 - \mathbf{r}/2) u_D^\dagger(\mathbf{r}_1 - \mathbf{r}/2) \\ + \mathbf{v}_D^\dagger(\mathbf{r}_1 - \mathbf{r}/2)] , \end{aligned} \tag{29a}$$

and

$$\begin{aligned} \mathbf{v}_D^\dagger(\mathbf{r}_1 - \mathbf{r}_2) \equiv N_1 \int d^3 r' \mathbf{r}' \exp(-i\mathbf{q} \cdot \mathbf{r}') \\ \times \exp\left[-\frac{(\mathbf{r}_1 - \mathbf{r}/2 + \mathbf{r}')^2}{R^2} \right] \\ \times \frac{m_+}{4\pi} \tilde{Y}_0(m_+ r') . \end{aligned} \tag{29b}$$

In practice, we tabulate these functions numerically for different values of the arguments and use linear interpolation at a later stage.

We are now ready to turn our attention back to the multidimensional integral specified by Eq. (20). We note that the integration with respect to $\mathbf{r}_4$ can be carried out analytically to yield Gaussian functions in $\mathbf{k}_4$ and then the integration with respect to $\mathbf{k}_4$ can be simplified to a one-dimensional integral. We obtain

$$G(|\mathbf{r}_1+\mathbf{r}/2|) \equiv \int \frac{d^3k}{(2\pi)^3}\frac{\exp[-ik(r_1+r/2)-k^2R^2/8]}{k^2+m_\pi^2-i\epsilon} = \frac{1}{2\pi^2|\mathbf{r}_1+\mathbf{r}/2|}\times\int_0^\infty \frac{\sin(|\mathbf{k}|\,|\mathbf{r}_1+\mathbf{r}/2|)\exp(-k^2R^2)}{k^2+m_\pi^2-i\epsilon}k^2dk\ , \tag{30}$$

so that the simplified result of $f_j^\pi(\mathbf{r},s)$ can be written as follows:

$$f_j^\pi(\mathbf{r},s) = -\frac{\zeta}{2}N_4^2N_1(\pi/2)^{3/2}R^5(2E_\pi)^{-1/2}g_{Q\pi}^3 \times\int d^3r_1\chi_{4f}^\dagger F(|\mathbf{r}_1+\mathbf{r}/2|)\chi_{4i}\phi^{(\pi)}(\mathbf{r}_1) \times\chi_{1f}^\dagger H(\mathbf{r}_1,\mathbf{r},\mathbf{q})\chi_{1i}\ , \tag{31}$$

with χ_1 and χ_4 the Pauli spinors of the two quarks. $F(|\mathbf{r}_1+\mathbf{r}/2|)$ and $H(\mathbf{r}_1,\mathbf{r},\mathbf{q})$ are given by

$$F(|\mathbf{r}_1+\mathbf{r}/2|) = \frac{i}{|\mathbf{r}_1+\mathbf{r}/2|}\times\frac{dG(|\mathbf{r}_1+\mathbf{r}/2|)}{d|\mathbf{r}_1+\mathbf{r}/2|}\boldsymbol{\sigma}\cdot(\mathbf{r}_1+\mathbf{r}/2) \tag{32a}$$

and

$$\begin{aligned}H(\mathbf{r}_1,\mathbf{r},\mathbf{q}) = \exp[-(\mathbf{r}_1-\mathbf{r}/2)^2/R^2] \times\Bigg\{&[m+(E_{1f}+E_\pi)-i\zeta\mathbf{q}\cdot(\mathbf{r}_1-\mathbf{r}/2)+\zeta\boldsymbol{\sigma}\cdot\mathbf{q}\times(\mathbf{r}_1-\mathbf{r}/2)]u_D^\dagger(\mathbf{r}_1-\mathbf{r}/2)\\ &+\left\{-\frac{\zeta^2R^2}{2}[-m+(E_{1f}+E_\pi)+\zeta][\mathbf{r}_1-\mathbf{r}/2-i\boldsymbol{\sigma}\times(\mathbf{r}_1-\mathbf{r}/2)]-\frac{i\zeta R^2}{2}(\mathbf{q}-i\boldsymbol{\sigma}\times\mathbf{q})\right\}\cdot\nabla_{r_1}u_D^\dagger(\mathbf{r}_1-\mathbf{r}/2)\\ &+\frac{\zeta R^2}{2}[\nabla^2\mathbf{u}_D^\dagger(\mathbf{r}_1-\mathbf{r}/2)+\nabla^2u_D(\mathbf{r}_1-\mathbf{r}/2)]+[m+(E_{1i}-E_\pi)]-i\zeta\mathbf{q}\cdot(\mathbf{r}_1-\mathbf{r}/2)\\ &+\zeta\boldsymbol{\sigma}\cdot(\mathbf{r}_1-\mathbf{r}/2)\times\mathbf{q}]u_D(\mathbf{r}_1-\mathbf{r}/2)+\left\{-\frac{\zeta^2R^2}{2}[-m+(E_{1i}-E_\pi)+\zeta][\mathbf{r}_1-\mathbf{r}/2+i\boldsymbol{\sigma}\times(\mathbf{r}_1-\mathbf{r}/2)]\right.\\ &\left.-\frac{i\zeta R^2}{2}(\mathbf{q}+i\boldsymbol{\sigma}\times\mathbf{q})\right\}\cdot\nabla_{r_1}u_D(\mathbf{r}_1-\mathbf{r}/2)\Bigg\}\ .\end{aligned} \tag{32b}$$

Incorporation of recoil corrections results in terms of order p/M or of order p^2/M^2 or higher with p the cluster momentum and makes Eqs. (31), (32a), and (32b) considerably more complicated. It is clear that we also need to simplify the expressions for the QI amplitudes due to the interactions $\tilde{V}_{16}\hat{P}_{36}$, $\tilde{V}_{36}\hat{P}_{36}$, and so on. In Appendix F of Ref. 12 a complete list of the simplified results for the various quark amplitudes is given.

At this juncture, it may be useful to examine the structure of Eqs. (31), (32a), and (32b). First of all, the amplitudes specified by these equations must be evaluated numerically for the various spin configurations as required by Eqs. (14a)–(14h). (Thus, we refer to these amplitudes as "spin amplitudes.") For a given configuration, we tabulate $u_D^\dagger, u_D$, and their derivatives so that the function $H(\mathbf{r}_1,\mathbf{r},\mathbf{q})$ can be evaluated numerically. As the next step, we use the tabulated functions F and H as the input to Eq. (31) [with F determined easily from Eqs. (32a) and (30)] and then combine the resultant three-dimensional integral with the two-dimensional angular integration required for the initial and final nucleon-nucleon wave functions [in the variable $\mathbf{r}$]. This last step requires an expression such as Eq. (16), which relates a partial wave amplitude to the various spin amplitudes.

In summary, the partial-wave amplitudes as illustrated by Eq. (16), *except* for the integration over dr, may now be evaluated and tabulated for the various choices of input parameters as follows:

(1) Three different pion kinetic energies, 82, 142, and 217 MeV, are chosen so that the elastic π-d scattering data can be used to extract an energy-dependent optical potential. This optical potential is used to generate the distorted S and P pion wave functions, which are used as an input in Eq. (31).

(2) At a given pion energy, we tabulate $u_D^\dagger$, u_D, and their derivatives [via Eqs. (26)–(28)] and use these tables with linear interpolation in calculating the functions such as $H(\mathbf{r}_1,\mathbf{r},\mathbf{q})$ [via Eq. (32b) and the formulae in Appendix

F of Ref. 12]. Note that the functions such as F [Eq. (32a)] can be determined easily.

(3) At a given pion energy, we calculate the spin amplitudes such as f_4^π, f_5^π, etc. [via, e.g., Eq. (31)], which depend on the nucleon-nucleon relative coordinates (r,θ,ϕ) and then, as indicated by Eq. (16), combine these spin amplitudes suitably to form partial-wave amplitudes. The net outcome is a list of partial-wave amplitudes tabulated as the functions of r.

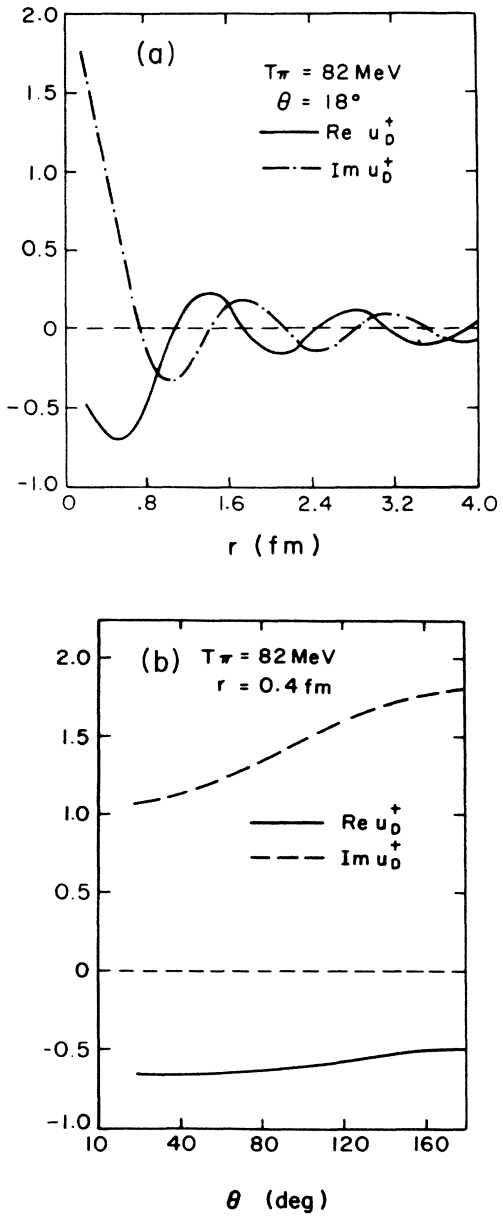

FIG. 4. Transformed quark wave functions by allowing the quark Feynman propagator to act on wave functions. Here we plot the result $u_D^\dagger$ vs (a) the radius r and (b) the angle between r and the Z axis. The quark mass is taken to be zero. Note also that both E_f and E_i are taken to be the quark eigenenergy, while the nucleon radius R is 0.572 54 fm (corresponding to $R_{\rm MIT}=0.8$ fm).

(4) Steps (1), (2), and (3) must be repeated for a given $NN\to NN\pi$ reaction of particular interest. In the present work, we focus on the reactions $p+p\to d+\pi^+$ and $n+p\to p+p+\pi^-$.

In closing this section we wish to emphasize that invocation of a relativistic quark model specified by Eqs. (21)—(24) allows us to simplify a large number of nontrivial 14-dimensional integrals (including the integration over d^3r) into five-dimensional integrals which can then be carried out numerically in an efficient manner via a quasi—Monte Carlo method.[16] If we choose to work directly with the quark wave function in the MIT bag,[15] it is not possible to have a similar simplification so that the amount of computing time required to make numerical predictions must be increased substantially.

III. NUMERICAL RESULTS

Assuming that pion production takes place effectively at the *quark* level and that quark-quark interactions are described to a sufficiently good approximation by one-gluon exchange plus *effective* one-pion exchange and the six-quark wave function is totally antisymmetrized, it is natural to group[12] the various reaction mechanisms at the hadronic level into several distinct categories, viz., (i) one-nucleon mechanism (ONM) or the nucleon-only impulse approximation (NOIA) where a pion is emitted from one of the two nucleon clusters [Fig. (1a)]; (ii) two-nucleon mechanisms (TNM) or meson-exchange currents (MEC) where pion emission takes place while the two nucleon clusters exchange a pion, and here we include isobar (Δ) currents [Fig. (1b)], ρ-π currents [Fig. (1d)], and pair currents [Fig. (1c)]; (iii) pion production with quark interchange [with or without boson exchange between two nucleon clusters]. We have described in Sec. II how the various contributions to the transition amplitude can be obtained. Specifically, it is shown that the quark-interchange (QI) amplitude can be simplified from an essentially 14-dimensional integral into a five-dimensional one. The central steps have been summarized at the end of Sec. II. In particular, we must tabulate, as functions of r, the partial-wave amplitudes as illustrated by Eq. (16) (*except* for the integration over dr) for the various choices of input parameters, including different pion kinetic energies [which are chosen to be 82, 142, and 217 MeV so that the elastic π-d scattering data can be used to extract an energy-dependent optical potential], the nucleon radius R, the strong coupling α_S^* $[=g_{QQ}^2/(4\pi)]$, and the effective pion-quark coupling α_π^* $[=g_{\pi Q}^2/(4\pi)]$. In what follows we wish to report a sample of numerical results on both the reactions $p+p\to d+\pi^+$ and $n+p\to p+p+\pi^-$.

As indicated earlier, we have adopted a quasi—Monte Carlo method[16] to carry out the five-dimensional integrals involved in the various partial-wave amplitudes. The precision and stability of this technique have been tested by varying the number N of integration steps as well as by using the method to do integrals with known integrated analytical results. A sample result is illustrated in Table II. It is clear that the integrated values do not vary very much from $N=10\,000$ up to $N=200\,000$. Subsequently,

TABLE II. Test of convergence of the Monte Carlo integration method versus the integration step number N. In obtaining the tabulated numbers, we have chosen the parameters as follows: the bag radius $R=0.429$ fm, and the coupling constant $\alpha_\pi=1$. f_s^π is the spin amplitude ($\uparrow\uparrow\rightarrow\uparrow\uparrow$ in this case) for an s-wave pion arising from one-pion exchange with quark interchange. The pion kinetic energy is 82 MeV.

N	f_s^π (np$\rightarrow\pi^-$pp) ($\times10^{-3}$)	f_s^π (pp$\rightarrow\pi^+$d) ($\times10^{-4}$)
5000	$-0.196-0.521i$	$-1.14-5.97i$
10000	$-0.239-5.03i$	$-0.939-6.38i$
20000	$-0.241-4.98i$	$-0.940-6.36i$
30000	$-0.247-4.97i$	$-0.942-6.37i$
50000	$-0.244-5.00i$	$-0.943-6.39i$
100000	$-0.245-5.00i$	$-0.937-6.39i$
200000	$-0.246-5.00i$	$-0.937-6.39i$

the integration step number N has been taken to be 10000 in our code, so that numerical results with accuracies better than 5% can be obtained with reasonable amounts of computing time.

To take into account effects caused by pion distortions, we choose a π-d optical potential which best fits the observed elastic π-d scattering data at three pion kinetic energies, 82, 142, and 217 MeV. This optical potential is chosen to be of the Kisslinger form,

$$V_{\pi d}(r)=-Ak^2b_0\rho(r)+Ab_1\nabla\cdot\rho(r)\nabla \tag{33a}$$

with A the mass number of the nucleus, k the pion momentum (in the pion-nucleus c.m. frame), $\rho(r)$ the nuclear density, and b_0 and b_1 some complex parameters. Specifically, $\rho(r)$ is taken as

$$\rho(r)=2(Zw^3\pi\sqrt{\pi})^{-1}\left[1+\frac{(Z-2)}{3}(r/w)^2\right]\times\exp(-r^2/w^2)\,, \tag{33b}$$

with $Z=1$ for the deuteron, and the size parameter of the nucleon density $w=1.39$ fm. The parameters b_0 and b_1 for πd$\rightarrow\pi$d elastic scattering at $T_\pi=82$, 142, and 217 MeV are found by fitting the data of Gabathuler *et al.*[17] as follows:

$$b_0=-3.75+0.994i,\quad b_i=4.71+0.115i\,,\quad \text{at } T_\pi=82 \text{ MeV}\,,$$
$$b_0=-2.397-0.829i,\quad b_1=7.499+0.534i\,,\quad \text{at } T_\pi=142 \text{ MeV}\,, \tag{33c}$$
$$b_0=-3.14-0.56i,\quad b_1=5.80+4.962i\,,\quad \text{at } T_\pi=217 \text{ MeV}\,.$$

In Figs. (5a)–(5c) we present the calculated cross section angular distributions at various pion kinetic energies. The χ^2 per degree of freedom for these fits are, respectively, 0.485, 7.17, and 29.17. We find some difficulty in reducing the χ^2 for $T_\pi=142$ MeV and 217 MeV mainly due to the failure at large angles, and the χ^2 cannot be reduced appreciably by a readjustment of $\rho(r)$. It turns out that, since the χ^2 are extremely sensitive to both b_0 and b_1, the resultant optical potential can be reliably pinned down once $\rho(r)$ is chosen.

We turn our attention to the predicted cross sections for both the reactions p+p$\rightarrow$d+π^+ and n+p$\rightarrow$p+p+π^-, respectively, in Figs. (6a) and (6b) and (7a) and (7b). In making these predictions, we have used the following input parameters:

$f=-0.996$ (pseudovector πNN coupling),

$g_\Delta=1.909$ (for isobar currents),

$g_{\rho NN}=2.326,\quad f_{\rho\pi\pi}=-0.646$ [for ($\rho\pi$) current]

from Ref. 13;

$$\Gamma_\Delta=(0.35/6)(q^{*3}/m_\pi^2)[(M^*+M)^2-m_\pi^2]M^{*-2}\,,$$

with

$$q^*=q_\pi\left[1-\frac{E_\pi}{2(M+E_\pi)}\right]\,, \tag{34}$$

for isobar currents, from Ref. 14; and

$R=0.572$ fm (corresponding to $R_{\rm MIT}=0.8$ fm),

$\alpha_S^*=1.97$,

α_π^* ($r=0$)$=0.31$ and α_π^* ($r=\infty$)$=3.572$

for quark-interchange mechanisms, from Refs. 18 and 19. It should be kept in mind that all these parameters are determined by other means and none of them have been readjusted to fit the p+p$\rightarrow$d+π^+ data.

In Figs. (6a) and (6b) the calculated cross section for the pion-absorption reaction π^+d$\rightarrow$p+p and the analyzing power A_y for the reaction $\vec{\rm p}$+p$\rightarrow$d+π^+ at $T_{\rm p}=180$ MeV are shown, respectively, as a function of η ($=q_\pi/m_\pi$) and as a function of the pion scattering angle $\theta_{\rm c.m.}$ (in the c.m. frame). In both figures we compare the prediction calculated with quark-interchange (QI) reaction mechanisms with that calculated without QI (NO QI). The p-p partial waves included in the calculations are $^3P_1$, $^1S_0$, and $^1D_2$. Although the importance of QI varies with the kinematic region, these two figures alone already confirm the observation made by Miller and Kisslinger[11] that

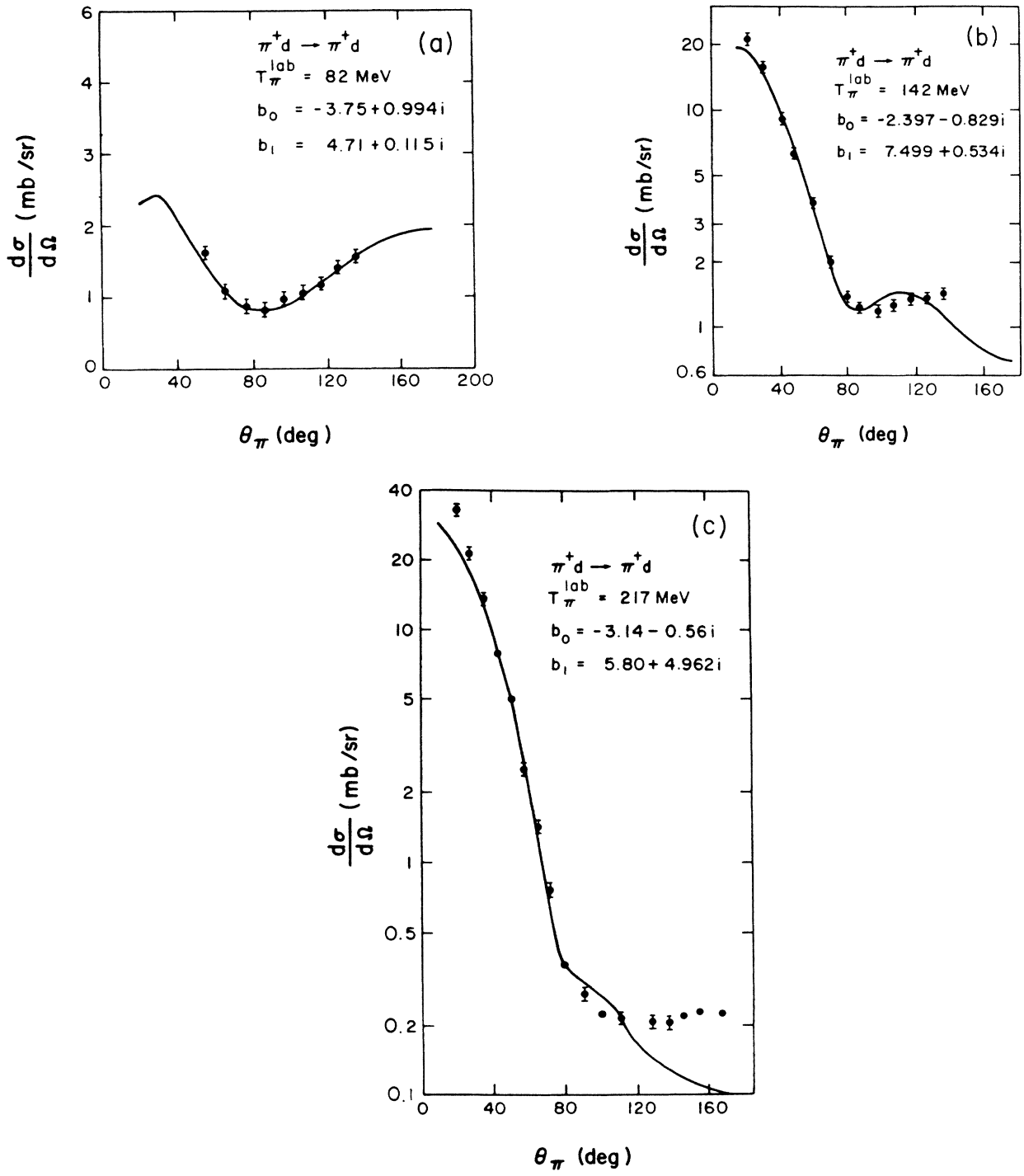

FIG. 5. Calculated differential cross sections for π^+d elastical scattering at the pion kinetic energies of (a) 82 MeV, (b) 142 MeV, and (c) 217 MeV with the best-fitted optical potentials. The data are from Ref. 17.

effects caused by short-distance quark-interchange mechanisms need to be considered even near the pion production threshold.

In Figs. (7a) and (7b) the predicted double differential cross section $d^3\sigma/dE_\pi d\Omega_\pi$ and the analyzing power A_y for the reaction $n+p \rightarrow p+p+\pi^-$ at the p-p excitation energy $E_x=4$ MeV and the pion emission angle $\theta_\pi=30°$ are both shown versus the initial proton energy $T_p^{c.m.}$. (Note that a neutron beam will likely be used in this experiment.) Specifically, we have included the following channels in these calculations: $^3P_0 \rightarrow {}^1S_0$, $^1S_0 \rightarrow {}^3P_0$, $^3S_1+{}^3D_1 \rightarrow {}^3P_1$, $^3D_2 \rightarrow {}^3P_2$ (all for S-wave pions), and $^3S_1+{}^3D_1 \rightarrow {}^1S_0$, $^3P_1 \rightarrow {}^3P_0$, $^3P_J \rightarrow {}^3P_1$, $^3P_J \rightarrow {}^3P_2$ (all for P-wave pions) for ONM (or NOIA) and TNM; $^3P_0 \rightarrow {}^1S_0$

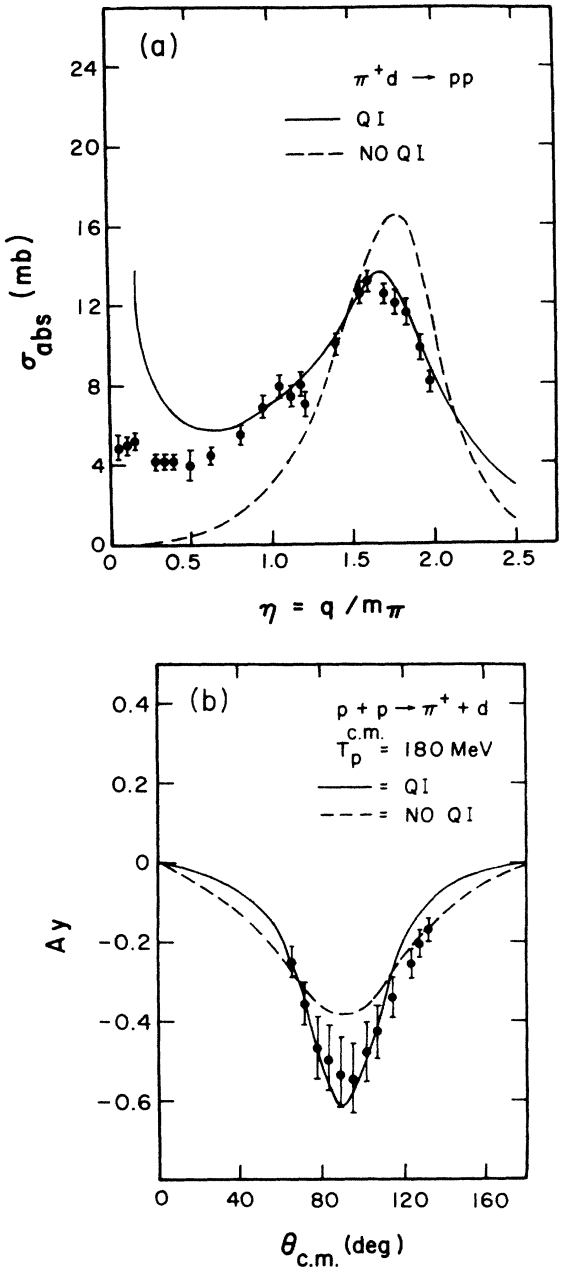

FIG. 6. (a) Calculated cross section for the pion-absorption reaction $\pi^+ d \rightarrow p+p$ and (b) the analyzing power A_y for the reaction $\vec{p}+p \rightarrow d+\pi^+$ at $T_p = 180$ MeV are shown as functions of η ($=q_\pi/m_\pi$) and the pion scattering angle $\theta_{c.m.}$ (in the c.m. frame), respectively. In both figures we compare the prediction calculated with quark-interchange (QI) reaction mechanisms with that calculated without QI (NO QI). The p-p partial waves included in the calculations are $^3P_1$, $^1S_0$, and $^1D_2$. The input parameters are listed in Eq. (34) in the text.

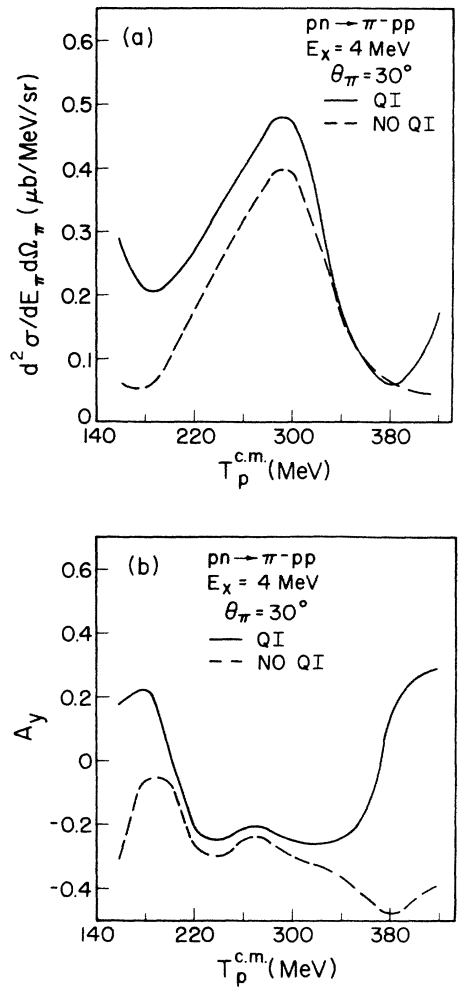

FIG. 7. Predicted (a) double differential cross section $d^2\sigma/dE_\pi d\Omega_\pi$ and (b) analyzing power A_y for the reaction $n+p \rightarrow p+p+\pi^-$ at the p-p excitation energy $E_x = 4$ MeV and the pion emission angle $\theta_\pi = 30°$ are both shown vs the initial proton energy $T_p^{c.m.}$. Specifically, we have included the following channels in the calculations: $^3P_0 \rightarrow {}^1S_0$, $^1S_0 \rightarrow {}^3P_0$, $^3S_1 + {}^3D_1 \rightarrow {}^3P_1$, $^3D_2 \rightarrow {}^3P_2$ (all for S-wave pions), and $^3S_1 + {}^3D_1 \rightarrow {}^1S_0$, $^3P_1 \rightarrow {}^3P_0$, $^3P_J \rightarrow {}^3P_1$, $^3P_J \rightarrow {}^3P_2$ (all for P-wave pions) for ONM (or NOIA) and TNM; $^3P_0 \rightarrow {}^1S_0$ and $^3S_1 + {}^3D_1 \rightarrow {}^1S_0$ for the various quark-interchange (QI) reaction mechanisms. The input parameters are listed in Eq. (34) in the text.

and $^3S_1 + {}^3D_1 \rightarrow {}^1S_0$ for the various quark-interchange (QI) reaction mechanisms. Once again, the numerical results show that effects due to quark-interchange reaction mechanisms should be included even near the pion production threshold. However, the optical potential for the π-(pp) system may differ significantly from the π-d optical potential. Results from a further investigation of this point, as reported in Ref. 12, suggest that our predictions for the reaction $n+p \rightarrow p+p+\pi^-$ are not modified severely by adoption of a rather different π-(pp) optical potential.

IV. SUMMARY

In this paper we have investigated pion production via nucleon-nucleon scattering, i.e., $N+N \rightarrow N+N+\pi$, assuming that pion emission takes place *effectively* at the quark level and that quark-quark interactions are described to a reasonable approximation by one-gluon ex-

change plus *effective* one-pion exchange. The six-quark wave function is totally antisymmetrized. Consequently, reaction mechanisms may be grouped into several categories: (1) one-nucleon mechanisms (ONM) or the nucleon-only impulse approximation (NOIA), (2) two-nucleon mechanisms (TNM) or meson-exchange currents (MEC), and (3) reaction mechanisms involving quark interchange (QI). Treatment of these reaction mechanisms has been sketched in some detail in Sec. II (with an extensive number of resultant formulas collected in Ref. 12). Applying the formalism to the reactions $p+p\rightarrow d+\pi^+$ and $n+p\rightarrow p+p+\pi^-$, we have found in Sec. III that, for a nucleon radius of about 0.8 fm (as used in the MIT bag model), reaction mechanisms involving quark interchange may be as important as the conventional one-nucleon or two-nucleon reaction mechanisms even near the pion production threshold. This result provides quantitative support of the conclusion reached by Miller and Kisslinger[11] from a hybrid quark-baryon model concerning the necessity of incorporating quark effects in describing pion production or absorption reactions.

ACKNOWLEDGMENTS

We wish to thank Professor G. A. Miller, Professor L. S. Kisslinger, and Professor G. E. Walker for valuable discussions and Professor R. D. Bent for encouragement. This work was supported in part by the National Science Foundation and in part by the U.S. Department of Energy.

[1] *Pion Production and Absorption in Nuclei (Indiana University, 1981)*, Proceedings of the Conference on Pion Production and Absorption in Nuclei, AIP Conf. Proc. No. 79, edited by Robert D. Bent (AIP, New York, 1982).

[2] S. E. Vigdor *et al.*, Phys. Rev. Lett. **49**, 1314 (1982); Nucl. Phys. **A396**, 61c (1983).

[3] P. Walden *et al.*, Phys. Lett. **B81**, 156 (1979); E. Aprile *et al.*, Nucl. Phys. **A335**, 245 (1980).

[4] M. D. Corcoran *et al.*, Phys. Lett. **B120**, 309 (1983).

[5] B. D. Keister and L. S. Kisslinger, Nucl. Phys. **A412**, 301 (1984); M. Dillig, J. S. Conte, and R. D. Bent, IUCF Annual Report No. 25, 1985 (unpublished); M. J. Iqbal and G. E. Walker, Phys. Rev. C **32**, 556 (1985).

[6] See Ref. 1, p. 65.

[7] B. Blankleider and I. R. Afnan, Phys. Rev. C **24**, 1572 (1981); M. Betz and T.-S. H. Lee, *ibid.* **23**, 375 (1981); A. S. Rinat and Y. Starkand, Nucl. Phys. **A397**, 381 (1983).

[8] W. M. Kloet and R. R. Silbar, Nucl. Phys. **A338**, 281 (1980); **A338**, 317 (1980); J. Dubach *et al.*, Phys. Lett. **B106**, 29 (1981); J. Phys. G **8**, 475 (1982).

[9] W. Kubodera *et al.*, J. Phys. G **6**, 171 (1980).

[10] R. R. Silbar, Comments Nucl. Part. Phys. **12**, 177 (1984).

[11] G. A. Miller and L. S. Kisslinger, Phys. Rev. C **27**, 1669 (1983).

[12] Z.-J. Cao, Ph.D. thesis, Indiana University, 1986.

[13] W-Y. P. Hwang and G. E. Walker, Ann. Phys. (N.Y.) **159**, 118 (1985).

[14] H. Sugawara and F. von Hippel, Phys. Rev. **172**, 1764 (1968).

[15] A. Chodos, R. L. Jaffe, K. Johnson, C. B. Thorn, and V. F. Weisskopf, Phys. Rev. D **9**, 3471 (1974); A. Chodos, R. L. Jaffe, K. Johnson, and C. B. Thorn, *ibid.* **10**, 2599 (1974). T. DeGrand, R. L. Jaffe, K. Johnson, and J. Kiskis, *ibid.* **12**, 2060 (1975).

[16] Masaaki Sugihara and Kazuo Murota, Math. Comput. **39**, 549 (1982).

[17] K. Gabathuler *et al.*, Nucl. Phys. **A350**, 253 (1980); C. R. Ottermann *et al.*, Phys. Rev. C **32**, 928 (1985).

[18] W-Y. P. Hwang, Ann. Phys. (N.Y.) (to be published).

[19] W-Y. P. Hwang, Phys. Rev. D **31**, 2826 (1985).